Proceedings of the 17th World Congress
The International Federation of Automatic Control
Seoul, Korea, July 6-11, 2008

Control of a Semi-Active MR-Damper Suspension System: A New Polynomial Model

Arjon Turnip*, Keum-Shik Hong* and Seonghun Park*

** School of Mechanical Engineering, Pusan National University; 30 Jangjeon-dong, Gumjeong-gu, Busan 609-735, Korea. (Tel: +82-51-510-2454; Fax: +82-51-514-0685; e--mail: kshong@ pusan.ac.kr)*

Abstract: In this paper, numerical aspects of a sensitivity control for the semi-active suspension system with a magneto-rheological (MR) damper are investigated. A 2-dof quarter-car model together with a 6th order polynomial model for the MR damper are considered. For the purpose of suppressing the vertical acceleration of the sprung mass, the square of the vertical acceleration is defined as a cost function and the current input to the MR damper is adjusted in the fashion that the current is updated in the negative gradient of the cost function. Also, for improving the handling performance, a weighted absolute velocity of the sprung mass is added to the control law. The implementation of the proposed algorithm requires only the measurement of the relative displacement of the suspension deflection. The local stability of the equilibrium point of the closed loop nonlinear system is proved by investigating the eigenvalues of the linearized one. Through simulations, the passive suspension, the skyhook control, and the proposed sensitivity control are compared.

1. INTRODUCTION

The use of magneto-rheological (MR) fluids is widely spreading in industrial applications: car suspension, seat suspension, bridge vibration control, washing machine vibration control, and gun vibration control. This paper focuses on a sensitivity control (a type of gradient approach) in adjusting the current input to the MR damper that is used in a car suspension system (Choi et al., 2001; Lee and Choi, 2001; Liu et al., 2006; Song et al., 2005)

The semi-active suspension system uses a varying damping force as a control force. For example, a hydraulic continuous-damping-control (CDC) damper varies the size of an orifice in the hydraulic flow valve to generate desired damping forces. An electro- rheological (ER) damper or a magneto-rheological (MR) damper applies various levels of electric field or magnetic field to cause various viscosities of the ER or MR fluids (Song et al., 2005; Liu et al., 2006; Park and Jung, 2003; Lee and Jeon, 2002; Park and Jeon, 2002). On the other hand, the fully active suspension system produces the control force with a separate hydraulic/pneumatic unit. Therefore, the cost and the weight of a fully active suspension system become obstacles in medium size cars. Comparing the three, a semi-active system is simpler and uses less energy than an active system, but provides better vibration isolation capability than a passive system at the sprung mass resonance frequency. The inferior performance of a semi-active suspension than an active one comes from the fact that the control force can be generated only when the desired control force and the damping have the same direction. From this view, semi-active suspension systems draw more attention because of their low cost and competitive performance to the fully active ones (Alleyne and Hedrick, 1995, Yi and Hedrick, 1995; Lin and Kanellakopoulos, 1997; Hong et al., 2002; Yi and Song, 1999; Karnopp and Crosby, 1974).

For a fixed suspension spring constant, the better isolation of the car body from the road disturbances can be achieved with a soft damping by allowing a larger suspension deflection. However, the better road contact can be achieved with a hard damping by not allowing unnecessary suspension deflections. Therefore, the ride quality and the handling performance of vehicle are two conflicting criteria in the control system design of suspension systems.

The skyhook control strategy was introduced by Karnopp et al. (1974). The skyhook control can reduce the resonant peak of the sprung mass quite significantly and thus achieve a good ride quality. But, in order to improve both the ride quality and the handling performance of the vehicle, the resonant peaks of both the sprung mass and the unsprung mass need to be reduced. However, the skyhook damper alone cannot reduce both resonant peaks at the same time. The implementation of a skyhook control (Lee and Jeon, 2002) needs two information: the absolute velocity of the sprung mass and the relative velocity between the sprung and unsprung masses. In this paper, the measurement of only the suspension relative displacement between the sprung and unsprung masses and the use of a MR damper are assumed. The damping force of the MR damper is modeled as a 6th order polynomial equation of the relative velocity with coefficients as affine functions of input current. The current input to the MR damper is adjusted, in principle, in the negative direction of the gradient vector of the square of the vertical acceleration of the sprung mass, but considering the handling performance a weighted absolute value of the sprung mass velocity has been added in the law. The stability of the proposed nonlinear control law has been analyzed at an equilibrium point.

2. MODELING: QUARTER CAR AND MR DAMPER

2.1 A quarter car model

Fig. 1 depicts a quarter-car model, where z_s, z_u, and z_r are the sprung-mass, the unsprung-mass, and the road displacements, respectively. The values of the parameters in this model are collected in Table 1. The control strategy is to adjust the damping force f_{mr} properly by applying the desired current input I to the MR damper, whereas the relative displacement $z_s - z_u$ is measured. Besides the intrinsic vertical motions limited to this quarter model, other issues such as the pitch and roll controls of the vehicle are not discussed in this paper. The equations of motion are

$$m_s \ddot{z}_s + k_s(z_s - z_u) + f_{mr}(\dot{z}_s - \dot{z}_u, I) = 0, \tag{1}$$

$$m_u \ddot{z}_u + k_u(z_u - z_d) - k_s(z_s - z_u) - f_{mr}(\dot{z}_s - \dot{z}_u, I) = 0, \tag{2}$$

where f_{mr} is given as a function of the relative velocity $\dot{z}_s - \dot{z}_u$ and the current input I. It is again remarked that only the relative displacement $z_s - z_u$ is measured.

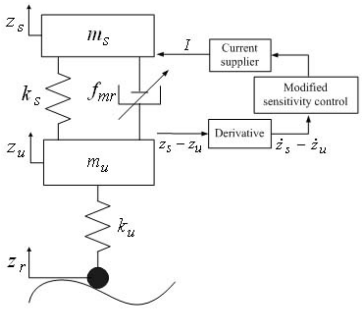

Fig. 1 1/4 car model.

Table 1. Nominal parameter values used in simulation.

Parameters	definitions	values
m_s	Sprung mass	460 kg
m_u	Unsprung mass	36 kg
k_s	Coil spring constant	28,000 N/m
k_u	Tire spring constant	186,000 N/m

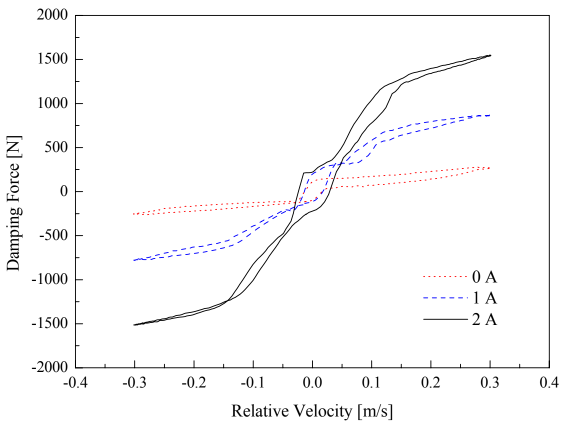

Fig. 2 Hysteresis curves of the used MR damper when $\dot{z}_s - \dot{z}_u = 0.3\cos 7.5t$

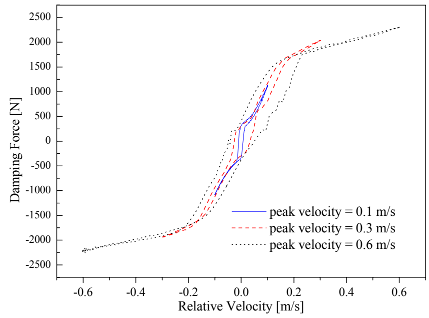

Fig. 3 Hysteresis curves for three sinusoidal relative displacements with 3 A current input.
($z_s - z_u = 0.04\sin 2.5t$, $0.04\sin 7.5t$, $0.04\sin 15t$, and $I = 3\,A$)

2.2 MR damper modelling

The semi-active dampers include the hydraulic discrete damping control damper using a step motor, the hydraulic continuous variable damper (CVD) using a solenoid valve, the ER damper, and the MR damper. The use of hydraulic dampers might be suitable for suppressing 1-4 Hz road disturbances, but may not be suitable for suppressing higher frequencies. Since the fluid used in an ER or MR damper has a fast response time, it can be used in a broader range of road condition. Also, the MR damper is known to be most suitable for car application since the strength of a MR fluid is 20-50 times higher than that of an ER damper and the less performance degradation due to impurities and precipitation is being reported. One notable feature of MR fluids is the hysteresis characteristics appearing in the expansion and contraction processes. Among the various models available in the literature, the model of Bingham is known simple, but it may not fully characterize the hysteresis behavior; the model of Bouc-Wen needs a very small step size when solving a stiff differential equation numerically; the nonparametric model of Song et al. (2005) might be another potential candidate (Bouc, 1967; Wen, 1975; Bingham, 1992).

In this paper, an algebraic approach rather than a differential equation approach is pursued. Fig. 2 shows three hysteresis curves in association with three current inputs, for a typical MR damper, when $0.3\cos 7.5t$ $(i.e., z_s - z_u = 0.04\sin 7.5t)$. It is seen that the damping force gets larger as the relative velocity gets larger. Also, the slope gets steeper as the current input gets bigger. However, it is seen that, for a fixed current input, the damping forces follow different curves in the expansion (the lower curve) and contraction (the upper curve) regions, which is a hysteresis effect.

On the other hand, for a fixed current input at 3 A, Fig. 3 shows three different hysteresis curves in association with three different sinusoidal relative-displacement profiles with the same magnitude but different frequencies, that is, $z_s - z_u$ = 0.04 sin 2.5t, 0.04 sin 7.5t, and 0.04 sin 15t. By differentiating them, $\dot{z}_s - \dot{z}_u =$ $0.1\cos 2.5t$, $0.3\cos 7.5t$ and $0.6\cos 15t$ are obtained, which correspond to three peak velocities 0.1, 0.3, and 0.6 m/s. The strategy in this paper is, instead of considering two hysteric curves in the expansion and contraction regions, to consider the peak damping forces at individual peak-velocity points. In this case, one polynomial equation for a given current input (representing the peak damping forces) will become sufficient in representing the damping force characteristics as follows:

$$f_{mr}(\dot{z}_s - \dot{z}_u, I) = \sum_{k=0}^{n} (a_k^{\circ} + b_k^{\circ}\ I\ ) (\dot{z}_s - \dot{z}_u)^k, \qquad n = 6 \tag{3}$$

where n is the order of the polynomial (n =6 is used in this paper) and a_k^0 and b_k^0 are the coefficients that should be determined through experiments. Fig. 4 shows seven such curves corresponding to seven different current inputs, where the lowest slope can be counted as the passive one with 0 current input. Table 2 shows a typical combination of the coefficients obtained from experiments for a SM_FRONT_Left MR CDC damper of Daewoo Precision Industries, Ltd., Korea. Fig. 5 depicts the experimental test bed using an MTS system. Fig. 6 demonstrates the closeness between experimental data and the values calculated from the polynomial model of (3) for three different current inputs: 0, 1, and 2 A.

Table 2. Coefficients a_k° and b_k° in (3) obtained from experimental data using the peak values

Coefficients	Values	Coefficients	Values
a_0°	0	b_0°	11.6
a_1°	989.1	b_1°	1228.5
a_2°	17.4	b_2°	-56
a_3°	-316.3	b_3°	-970.5
a_4°	19	b_4°	52.2
a_5°	98.1	b_5°	254.3
a_6°	1.1	b_6°	-16.9

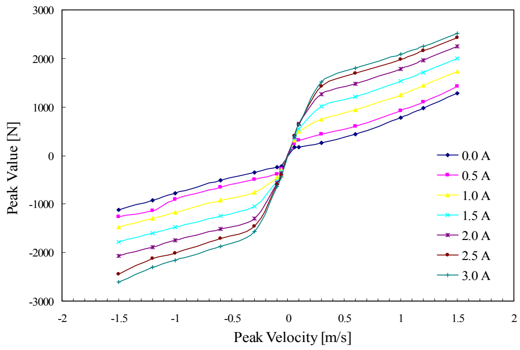

Fig. 4 Peak values of a typical MR CDC damper for various current inputs

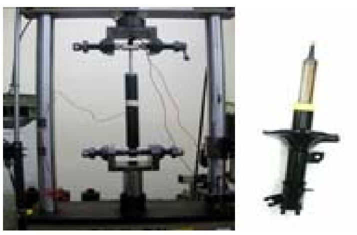

Fig. 5 Damping force measurement with an MTS System

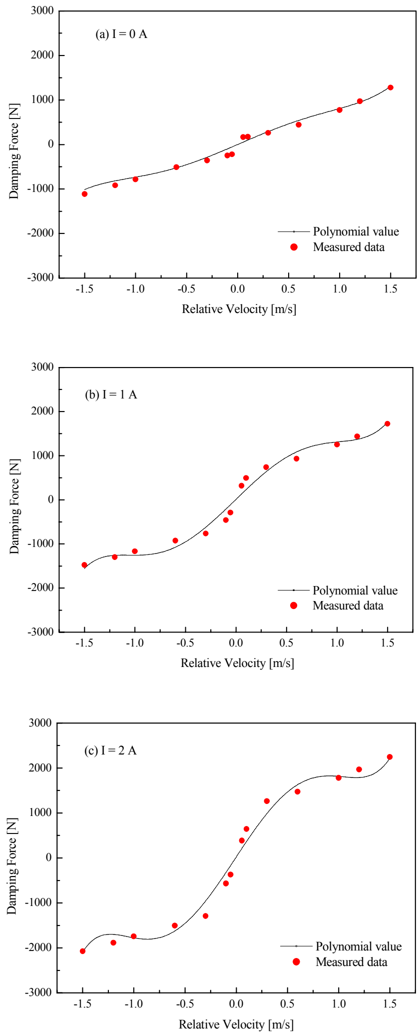

Fig. 6 Comparison between measured data and polynomial model (3).

3. SENSITIVITY CONTROL

In this paper, measurement of the relative displacement is assumed. In this case, it is known that an identification of the sprung mass and the coil spring constant is not possible.

3.1 Control law

The square of the vertical acceleration is considered as a performance criterion to be minimized as follows.

$$J = \ddot{z}_s^2 \,. \tag{4}$$

Observing (1), it is remarked that $\ddot{z}_s$ is a function of I (of course, it is also a function of other variables and parameters). For computing the current input, the following control law with two adjustable parameters is proposed as follows.

$$\dot{I} = -\mu_1 \frac{\partial J}{\partial I} + \mu_2 |\,\dot{z}_s\,| \,, \tag{5}$$

where I is updated in the negative gradient of J with a weighting μ_1, and $\mu_2 |\,\dot{z}_s\,|$ is an additional term that has been introduced to improve the handling performance of the vehicle on purpose. Such situations that the ride quality is less important will be addressed in Section 3.3. To implement (5), two values are needed: $\partial J / \partial I$ and $|\dot{z}_s|$. The first term is calculated as follows.

$$\frac{\partial J}{\partial I} = 2\ddot{z}_s \frac{\partial \ddot{z}_s}{\partial I}, \tag{6}$$

in which $\partial \ddot{z} / \partial I$ is the sensitivity of the vertical acceleration with respect to I. In Section 3.2 below, detailed derivations are given. On the other hand, $\ddot{z}_s$ can be estimated using (1) as follows.

$$\ddot{z}_s = -\frac{1}{m_s}\{ k_s(z_s - z_u) + f_{mr}(\dot{z}_s - \dot{z}_u, I) \}. \tag{7}$$

Again, $\dot{z}_s$ can be calculated by integrating (7).

3.2 Sensitivity calculation

The differentiation of (1) with respect to I yields.

$$m_s \frac{d\ddot{z}_s}{dI} + k_s \frac{d(z_s - z_u)}{dI} + \frac{d}{dI} f_{mr}(\dot{z}_s - \dot{z}_u, I) = 0. \tag{8}$$

The last term in (8) can be split into two parts as follows.

$$\frac{d}{dI} f_{mr}(\dot{z}_s - \dot{z}_u, I) = \frac{\partial f_{mr}}{\partial(\dot{z}_s - \dot{z}_u)} \frac{d(\dot{z}_s - \dot{z}_u)}{dI} + \frac{\partial f_{mr}}{\partial I}. \tag{9}$$

Using (3), $\partial f_{mr} / \partial(\dot{z}_s - \dot{z}_u)$ and $\partial f_{mr} / \partial I$ can be written as follows.

$$\frac{\partial f_{mr}}{\partial(\dot{z}_s - \dot{z}_u)} = \sum_{k=1}^{6} k(a_k^\circ + b_k^\circ I)(\dot{z}_s - \dot{z}_u)^{k-1}, \tag{10}$$

$$\frac{\partial f_{mr}}{\partial I} = \sum_{k=0}^{6} b_k^\circ (\dot{z}_s - \dot{z}_u)^k. \tag{11}$$

Finally, one notable observation is that the displacement and velocity of the unsprung mass are not much affected by the current input I. This is because the spring coefficient of the tire is 10 times larger than that of the coil spring and the unsprung mass m_u is 1/10 of the sprung mass m_s. Hence, $d(\dot{z}_s - \dot{z}_u)/dI$ and $d(z_s - z_u)/dI$ can be computed as follows

$$\frac{d(\dot{z}_s - \dot{z}_u)}{dI} = \frac{d\dot{z}_s}{dI}, \tag{12}$$

$$\frac{d(z_s - z_u)}{dI} = \frac{dz_s}{dI}. \tag{13}$$

Using (9)-(13), (8) can be written as follows.

$$m_s \ddot{s} + \left\{ \sum_{k=0}^{6} k(a_k^\circ + b_k^\circ I)(\dot{z}_s - \dot{z}_u)^{k-1} \right\} \dot{s} + k_s s + \sum_{k=0}^{6} b_k^\circ I (\dot{z}_s - \dot{z}_u)^k = 0, \tag{14}$$

where $\ddot{s}$, $\dot{s}$ and s correspond to $d\ddot{z}_s/dI$, $d\dot{z}_s/dI$, and dz_s/dI, respectively. As a conclusion, the sensitivity $\ddot{s}$ appears in a second order differential equation, and by solving this, dJ/dI in (6) can be obtained. Finally, the control law (5) is given as follows.

$$\dot{I} = \mu_1 \frac{2}{m_s}\left\{ k_s(z_s - z_u) + \sum_{k=0}^{6} (a_k^\circ + b_k^\circ I)(\dot{z}_s - \dot{z}_u)^k \right\} \ddot{s} + \mu_2 |\dot{z}_s| \tag{15}$$

3.3 Effect of $\mu_2 |\dot{z}_s|$

As discussed earlier, the second term $\mu_2 |\dot{z}_s|$ in (6) has been added for the purpose of improving the handling performance of the vehicle. It is known that, in the case of a passive damper, that is, $F_{damper} = c_s(\dot{z}_s - \dot{z}_u)$, the resonant peak at near 1 Hz decreases as the damping coefficient c_s increases.

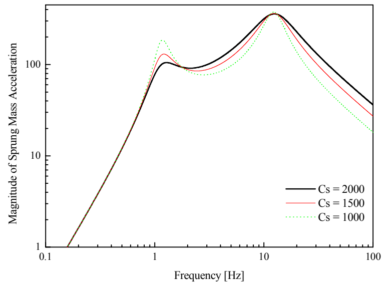

Fig. 7 Frequency responses of the sprung mass acceleration for three different damping coefficients (simulation results with the values in Table 1).

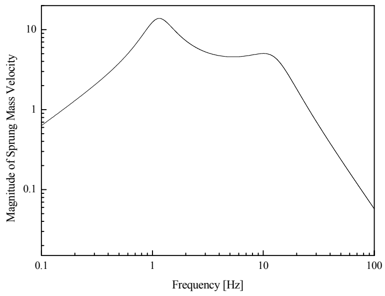

Fig. 8 Frequency response of the sprung mass velocity in the passive case of Fig. 7.

On the other hand, in the frequency range above 1 Hz, the sprung mass acceleration increases as the damping coefficient increases. Therefore, it is desirable to have a large damping coefficient at the resonant frequency and to have a small damping coefficient in the frequency range above the resonant frequency. Fig. 8 depicts the frequency response of the sprung mass velocity of a typical passive damper. As can be seen, the maximum magnitude of the sprung mass velocity appears at the resonant frequency of the sprung mass. Henceforth, by adding the term $\mu_2 |\dot{z}_s|$ in (6), such an effect of increasing the damping coefficient at the resonant frequency can be obtained.

4. STABILITY ANALYSIS

4.1 Figures and tables

In this section, the stability of the proposed control law in (15) is analyzed. The following state variables and state vector are defined.

$$x_1 = z_s - z_u, \ x_2 = \dot{z}_s, \ x_3 = z_u - z_r, \ x_4 = \dot{z}_u, \ x_5 = I, \ x_6 = s, \text{ and } x_7 = \dot{s}, \tag{16}$$

$$X = [x_1 \ x_2 \ x_3 \ \ldots \ x_7]^T. \tag{17}$$

Using (16), the state equations including (1), (2), (3), (6) and (15) are given as follows.

$$\dot{x}_1 = \dot{z}_s - \dot{z}_u = x_2 - x_4 \equiv f_1(X,t), \quad (18)$$

$$\dot{x}_2 = \ddot{z}_s = -\frac{1}{m_s}\left\{ k_s x_1 + \sum_{k=0}^{6}(a_k^{\circ} + b_k^{\circ} x_5)(x_2 - x_4)^k \right\} \quad (19)$$
$$\equiv f_2(X,t),$$

$$\dot{x}_3 = \dot{z}_u - \dot{z}_r = x_4 \equiv f_3(X,t), \quad (20)$$

since $z_r = 0$ can be assumed for stability analysis,

$$\dot{x}_4 = \ddot{z}_u = -\frac{1}{m_u}\{ -k_s x_1 + k_u x_3$$
$$- \sum_{k=0}^{6}(a_k^{\circ} + b_k^{\circ} x_5)(x_2 - x_4)^k \} \quad (21)$$
$$\equiv f_4(X,t),$$

$$\dot{x}_5 = \dot{I} = \mu_1 \frac{2}{m_s}\left\{ k_s x_1 + \sum_{k=0}^{6}(a_k^{\circ} + b_k^{\circ} x_5)(x_2 - x_4)^k \right\} \quad (22)$$
$$\cdot f_7(X,t) + \mu_2 |x_2| \equiv f_5(X,t),$$

$$\dot{x}_6 = \dot{s} = x_7 \equiv f_6(X,t), \quad (23)$$

$$\dot{x}_7 = \ddot{s} = -\frac{1}{m_s}\Big\{ x_7 \sum_{k=0}^{6}\left(a_k^0 + b_k^0 x_5\right)k\left(x_2 - x_4\right)^{k-1}$$
$$+ k_s x_6 + \sum_{k=0}^{6} b_k^0 \left(x_2 - x_4\right)^k \Big\} \quad (24)$$
$$\equiv f_7(X,t).$$

The equilibrium points from (18)-(24) are

$$x_1 = -\frac{a_0^{\circ} + b_0^{\circ} x_5}{k_s}, \quad x_2 = x_3 = x_4 = x_7 = 0, \quad (25)$$
$$x_5 = x_5(\text{any value}), \quad x_6 = -\frac{b_0^{\circ}}{k_s}.$$

Recall that x_5 denotes the current input in the range of [0, 3] A. Now, the linearization of equations (18)-(24) with respect to the equilibrium point $X_e = [-(a_0^{\circ} + b_0^{\circ} x_5)/k_s,\ 0,\ 0,\ 0,\ x_5,\ -b_0^{\circ}/k_s,\ 0]^T$ yields.

$$\dot{X} = \left.\frac{\partial F}{\partial X}\right|_{X_e} X, \quad (26)$$

where

$$\left.\frac{\partial F}{\partial X}\right|_{X_e} = \begin{bmatrix} 0 & 1 & 0 & -1 & 0 & 0 & 0 \\ -\frac{k_s}{m_s} & -\frac{a_1^{\circ} + b_1^{\circ} x_5}{m_s} & 0 & \frac{a_1^{\circ} + b_1^{\circ} x_5}{m_s} & -\frac{b_0^{\circ}}{m_s} & 0 & 0 \\ 0 & 0 & 0 & 1 & 0 & 0 & 0 \\ \frac{k_s}{m_u} & \frac{a_1^{\circ} + b_1^{\circ} x_5}{m_u} & -\frac{k_u}{m_u} & -\frac{a_1^{\circ} + b_1^{\circ} x_5}{m_u} & \frac{b_0^{\circ}}{m_u} & 0 & 0 \\ 0 & \mu_2 & 0 & 0 & 0 & 0 & 0 \\ 0 & 0 & 0 & 0 & 0 & 0 & 1 \\ 0 & -\frac{b_1}{m_s} & 0 & \frac{b_1}{m_s} & 0 & -\frac{k_s}{m_s} & -\frac{a_1^{\circ} + b_1^{\circ} x_5}{m_s} \end{bmatrix} \quad (27)$$

Observing the first, third, and fifth rows in (27), the existence of a linear dependence relationship among them can be seen. Hence, $\partial F / \partial X|_{X_e}$ has nullity 1 and any value in the nullspace can be an equilibrium point. Also, since $\partial F / \partial X|_{X_e}$ involves x_5, the eigenvalues of $\partial F / \partial X|_{X_e}$ is given as a function of x_5. Therefore, using MATLAB, the real parts of all eigenvalues can be computed. Fig. 9 shows that the real parts of all the eigenvalues are negative except one eigen value having zero real part. Therefore, the local stability is proved.

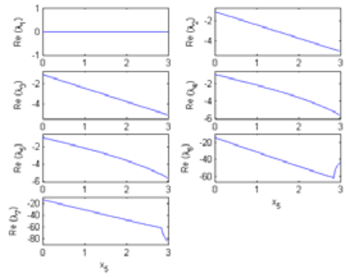

Fig. 9 Real parts of the eigenvalues of $\partial F / \partial X|_{Xe}$ over the range of x_5 (0~3 A)

5. SIMULATIONS

Three aspects are simulated: the role of the second term in (6), the performance of the sensitivity control law in comparison with the skyhook control, and the robustness of the proposed control algorithm against the variations of the sprung mass and coil spring constant.

5.1 The effect of $\mu_2 |\dot{z}_s|$

Fig. 10 compares the sprung mass acceleration of the sensitivity algorithm with $\mu_1 = 0.5$ and $\mu_2 = 0$ with that of a passive damper. As seen in Fig. 10, the performance of the sensitivity control is inferior in the lower frequency range. However, as seen in Fig. 11, by increasing μ_2 values, improved performances in the lower frequency range as well as in the high frequency range can be obtained. It is desirable to have a large μ_2-value below 3 Hz and to have a small μ_2-value above 3 Hz.

5.2 Comparison with the Skyhook Control

The skyhook control algorithm is given as follows (Alleyne and Hedrick, 1995).

$$f_{mr} = c_{sky}\dot{z}_s, \quad \text{if } \dot{z}_s(\dot{z}_s - \dot{z}_u) > 0, \quad c_{sky} = 1500,$$
$$f_{mr} = 0, \quad \text{if } \dot{z}_s(\dot{z}_s - \dot{z}_u) < 0. \quad (28)$$

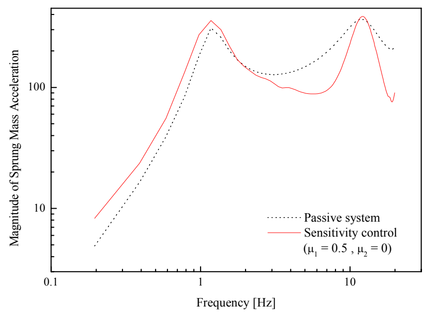

Fig. 10 Frequency responses of the sprung mass acceleration with μ_1=0.5 and μ_2=0

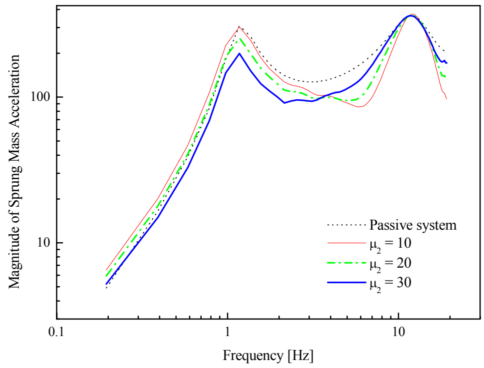

Fig. 11 Frequency responses of the sprung mass acceleration for various values of μ_2 (μ_1=0.5).

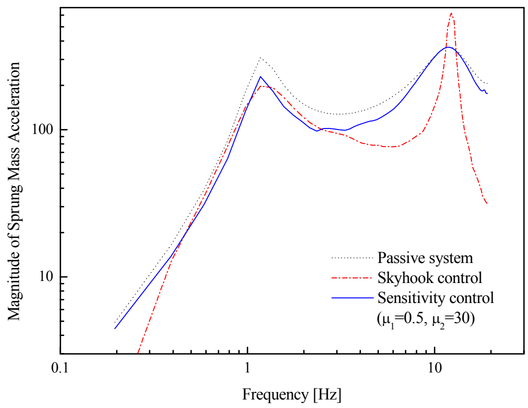

Fig. 12 Comparison of the frequency responses of the sprung mass acceleration.

Fig. 12 compares the passive damper, the skyhook control law with $c_{sky} = 1{,}500$, and the sensitivity control law with $\mu_1 = 0.5$ and $\mu_2 = 30$. At the resonant frequency, both the skyhook control and the sensitivity control show comparable performance, but at the resonant frequency of the unsprung mass of 11.7 Hz, the sensitivity control shows a comparable or better performance to the passive damper.

6. CONCLUSIONS

In this paper, to improve the ride quality at 1 Hz without sacrificing the handling performance, a sensitivity control law combining a negative gradient of the performance index and a weighted absolute velocity of the sprung mass was developed. The proposed algorithm demonstrated a comparable performance with the passive damper at the resonant frequency of the unsprung mass, but an improved performance of the ride quality at the resonant frequency of the sprung mass. It was desirable to have a large value of μ_2 at a low frequency road input, but to have a small value at a high frequency road input.

ACKNOWLEDGMENT

This work was supported by the Korean Research Foundation Grant funded by the Korean Government (MOEHRD, Basic Research Promotion Fund) (KRF-2007-314-D00011).

REFERENCES

Alleyne, A. and J. K. Hedrick (1995). Nonlinear adaptive control of active suspensions. *IEEE Transaction on Control Systems Technology*, **3**(1), 94-101.

Bingham, E. C. (1992). *Fluidity and Plasticity*, McGraw-Hill.

Bouc, R. (1967). Force vibration of mechanical systems with hysteresis. *4th on conf. on Nonlinear Oscillation*, Prague.

Choi, S. B., S. K. Lee, and Y. P. Park (2001). A hysteresis model for the field-dependent damping force of a magnetorheological damper. *Journal of Sound and Vibration*, **2**, 375-383.

Hong, K. S., H. C. Sohn, and J. K. Hedrick (2002). Modified skyhook control of semi-active suspension: A new model, gain scheduling, and hardware-in-the loop tuning. *ASME Transactions, Journal of Dynamic Systems, Measurement, and Control*, **124**(1), 158-167.

Karnopp, D. C., M. J. Crosby, and R. A. Harwood (1974). Vibration control using semi-active force generators. *ASME Journal of Engineering for Industry*, **96**(2), 619-626.

Lee, S. K. and S. B. Choi (2001). Hysteresis model of damping force of MR damper for a passenger car. *KSAE: The Korean Society Automotive Engineers*, **9**(1), 189-197.

Lee, Y. and D. Y. Jeon (2002). A study on the vibration attenuation of a driver seat using an MR fluid damper, Journal of Intelligent Material Systems and Structures, 13, 437-441.

Lin, J. S. and I. Kanellakopoulos (1997). Nonlinear design of active suspensions. *IEEE Control System Magazine*, **17**(3), 45-59.

Liu, Y. Q., H. Matsuhisa, H. Utsuno, and J. G.. Park (2006). Vibration control by a variable damping and stiffness system with magnetorheological dampers, *JSME International Journal Series C-Manufacturing*, **49**(2), 411-417.

Park, C. and D. Y. Jeon (2002). Semiactive vibration control of a smart seat with an MR fluid damper considering its time delay, Journal of Intelligent Material Systems and Structures, 13, 521-524.

Park, Y. and B. Jung (2003). Development of damper for new electronically controlled power-steering system by magneto-rheorogical fluid: MRSTEER, International Journal of Vehicle Design, **33**, 103-114.

Song, X., M. Ahmadian, S. Southward, and L. R. Miller (2005). An adaptive semiactive control algorithm for magnetorheological suspension systems. *ASME Journal Vibration Acoustics*, **127**, 493-502.

Wen, Y. K. (1975). Approximate method for non-Linear random vibration. *J. Engng Mech ASCE*, **102**(2), 249-263.

Yi, K. and J. K. Hedrick (1995). Observer-based identification of nonlinear system parameters. *ASME Trans., Journal of Dynamic Systems, Measurement, and Control*, **117**(2), 175-182.

Yi, K. S. and B. S. Song (1999). Observer design for semi-active suspension control, Vehicle System Dynamics, 32, 129-148.